Journal of *Marine Science and Engineering*

MDPI

Article

First Evidence of Contourite Drifts in the North-Western Sicilian Active Continental Margin (Southern Tyrrhenian Sea)

Daniele Spatola [1,2,*], Attilio Sulli [3], Daniele Casalbore [1] and Francesco Latino Chiocci [1]

[1] Department of Earth Sciences, Sapienza University, 00185 Rome, Italy; daniele.casalbore@uniroma1.it (D.C.); francesco.chiocci@uniroma1.it (F.L.C.)
[2] Department of Geosciences, University of Malta, Msida, MSD 2080, Malta
[3] Dipartimento di Scienze della Terra e del Mare, Università di Palermo, 90123 Palermo, Italy; attilio.sulli@unipa.it
* Correspondence: daniele.spatola@uniroma1.it

Abstract: We present the results of an integrated geomorphological and seismo-stratigraphic study based on high resolution marine data acquired in the north-western Sicilian continental margin. We document for the first time five contourite drifts (marked as EM1a, EM2b, EM2, EM3a, and EM3b), located in the continental slope at depths between ca. 400 and 1500 m. EM1a,b have been interpreted as elongated mounded drifts. EM1a,b are ca. 3 km long, 1.3 km wide, and have a maximum thickness of 36 m in their center that thins northwards, while EM1b is smaller with a thickness up to 24 m. They are internally characterized by mounded seismic packages dominated by continuous and parallel reflectors. EM2 is located in the upper slope at a depth of ca. 1470 m, and it is ca. 9.3 km long, more than 3.9 km wide, and has a maximum thickness of ca. 65 m. It consists of an internal aggradational stacking pattern with elongated mounded packages of continuous, moderate to high amplitude seismic reflectors. EM2 is internally composed by a mix of contourite deposits (Holocene) interbedded with turbiditic and/or mass flow deposits. EM1a,b and EM2 are deposited at the top of an erosional truncation aged at 11.5 ka, so they mostly formed during the Holocene. EM3a,b are ca. 16 km long, more than 6.7 km wide, and have a thickness up to 350 m. Both EM2 and EM3a,b have been interpreted as sheeted drift due to their morphology and seismic features. The spatial distribution of the contourite drifts suggests that the drifts are likely generated by the interaction of the LIW, and deep Tyrrhenian water (TDW) on the seafloor, playing an important role in the shaping this continental margin since the late Pleistocene-Holocene. The results may help to understand the deep oceanic processes affecting the north-western Sicilian continental margin.

Keywords: contourites; bottom currents; continental slope; moat; seismic reflection data; Mediterranean Sea

check for updates

Citation: Spatola, D.; Sulli, A.; Casalbore, D.; Chiocci, F.L. First Evidence of Contourite Drifts in the North-Western Sicilian Active Continental Margin (Southern Tyrrhenian Sea). *J. Mar. Sci. Eng.* **2021**, *9*, 1043. https://doi.org/10.3390/jmse9101043

Academic Editor: Alain Trentesaux

Received: 30 August 2021
Accepted: 20 September 2021
Published: 23 September 2021

Publisher's Note: MDPI stays neutral with regard to jurisdictional claims in published maps and institutional affiliations.

Copyright: © 2021 by the authors. Licensee MDPI, Basel, Switzerland. This article is an open access article distributed under the terms and conditions of the Creative Commons Attribution (CC BY) license (https://creativecommons.org/licenses/by/4.0/).

1. Introduction

Bottom currents play a key role in controlling the morphological and sedimentary evolution of continental margins, giving rise to a large spectrum of erosive and depositional morphologies [1–3]. Bottom currents are strongly influenced by a number of physical factors such as thermohaline circulation, tides, seafloor topography, and internal density drive pulses [4,5]. Bottom currents can transport large volumes of sediments [6,7] and build extensive (up to hundreds of kilometers long) and thick (up to few kilometers) sedimentary bodies called contourite drifts, which are generally oriented parallel to continental margins [1,8–10]. Evidence of large contourite drifts (or sediment drift) was documented and accurately described for the first time in the Northern and Southern Atlantic in the early 1960s [11], and since then similar drifts successively have been discovered in several oceans, seas, and even in lakes [12]. A growing number of studies focus on contourite drifts [1] since they can provide significant insights for paleo-oceanographic and paleo-climatic

reconstructions [4,13], hydrocarbon exploration [14,15], slope stability/geological hazard assessment [6,16–18], and recently for microplastic accumulation in deep-water [19].

Internal and external geometries of the contourite drifts are controlled by a number of factors such as seafloor morphology, current velocity, type and volume of available sediments, climate condition, and sea-level changes [8,20,21]. Based on their morphological and seismic features, Faugères et al. (1999) [8] and successively Rebesco et al. (2014) [1] proposed an accurate nomenclature to classify contourite drifts, including: (i) elongated mounded drifts, (ii) sheeted drifts, (iii) confined drifts, (iv) channel-related drifts, (v) fault-controlled drifts, (vi) patch drifts, (vi) infill drifts, and (vii) mixed drifts [1].

Elongated mounded drifts and sheeted drifts are the most widespread types of contourite drifts worldwide as well as in the continental margins of the central Mediterranean Sea [6,22–28]. Within the semi-enclosed and tectonically active central Mediterranean Sea, contourite systems are generally small and usually related to the path of the Levantine Intermediate Water (LIW, hereafter) [17,29–32].

In this study, we focus on the north-western part of the tectonically active Sicilian Continental Margin between the Castellammare Gulf and the Palermo Gulf (Figure 1), where several geomorphic elements associated with tectonic deformation, slope failure, and fluid seepage were identified, giving rise to a very complex morphology, [33–36]. Actually, the role played by bottom currents along this margin is still poorly known, except for a field of large-scale bedforms reported between 1000 and 1200 m water depth by Marani et al. (1993) [30], some tens of km to the east of our study area.

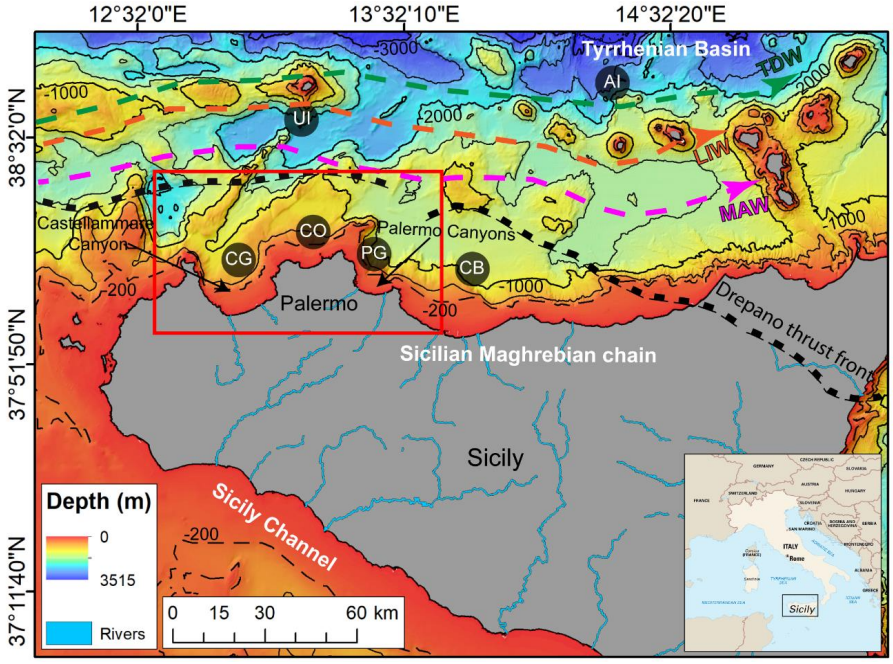


Figure 1. Location map of the study are showing the main morphological features, the distribution of the main pathways of water masses. Bathymetry interval: isobaths in black at 500 m intervals from 500 upward, and the dashed line indicates the 200 m isobath (shelf break). MAW: Modified Atlantic Water, LIW: Levantine Intermediate Water, TDW: Tyrrhenian Deep Water, CG: Castellammmare Gulf, CO: Offshore of Carini, PG: Palermo Gulf, CB: Cefalù Basin, UI: Ustica Island, AI: Aeolian Islands. Background bathymetry from EMODnet bathymetry (http://www.emodnet-bathymetry.eu, accessed on 15 August 2021).

By integrating high-resolution geophysical data (multibeam bathymetry and seismic profiles) and available sedimentological data, we: document, for the first time, evidence of contourite drifts, and decipher the role played by the bottom currents in the shaping of the upper part of the continental slope off NW Sicily. This area is crucial for geologic and palaeoceanographic reconstruction between the western and eastern Mediterranean Basins.

2. Regional Setting

2.1. Geological Setting

The north-western Sicilian Continental Margin (southern Tyrrhenian Sea; Figure 1), is located in the transitional area between the Sicilian Maghrebian chain to the south and the Tyrrhenian basin to the north [33,37–39]. This region originated as a consequence of a complex interaction of compressional events, crustal thinning and strike-slip faulting [37]. The Sicilian-Maghrebian Fold and Thrust Belt is a segment of the Apenninic-Maghrebian system formed by the convergence between Africa and Eurasian plates [40], and the contemporary roll-back of the Ionian slab [41–44]. Tectonic activity started since the early Miocene with the thrusting of the Kabilian-Calabrian units (along the Drepano thrust front, Figure 1) and the deformation of the internal units of the Sicilian-Maghrebian chain [37,41,45].

The seafloor morphology of the north-western Sicily Continental Margin is an alternation of morphostructural highs and depressed basins [34,37]. Its physiography is characterized by: (i) a narrow (less than 10 km wide) and steep (up to 3°) continental shelf; (ii) a very steep upper continental slope (up to 15°) between 150 and 1000 m; (iii) a nearly flat intra-slope basins located at a depth of ca. 1500 m; (iv) a lower continental slope, wider and gentler than the upper slope, at depths greater than 1000 m, and (v) a bathyal plain deeper than 3000 m [33,34,46]. The slope is characterised by a drainage network formed by a main submarine canyon (i.e., Castellammare Canyon) and more than two hundred tributaries variably oriented (Lo Iacono et al., 2014) [33].

The sediment distribution map in Figure 2, highlights the main feature classes of the seafloor sediments in the study area, where rocks outcrop only on the continental shelf in proximity of the promontories [47]. The inner continental shelf is dominated by sand, while its distal part by muddy sand. The continental slope is characterised by the predominance of sandy mud down to ca. 1000 m and by mud in the deeper region (Figure 2).

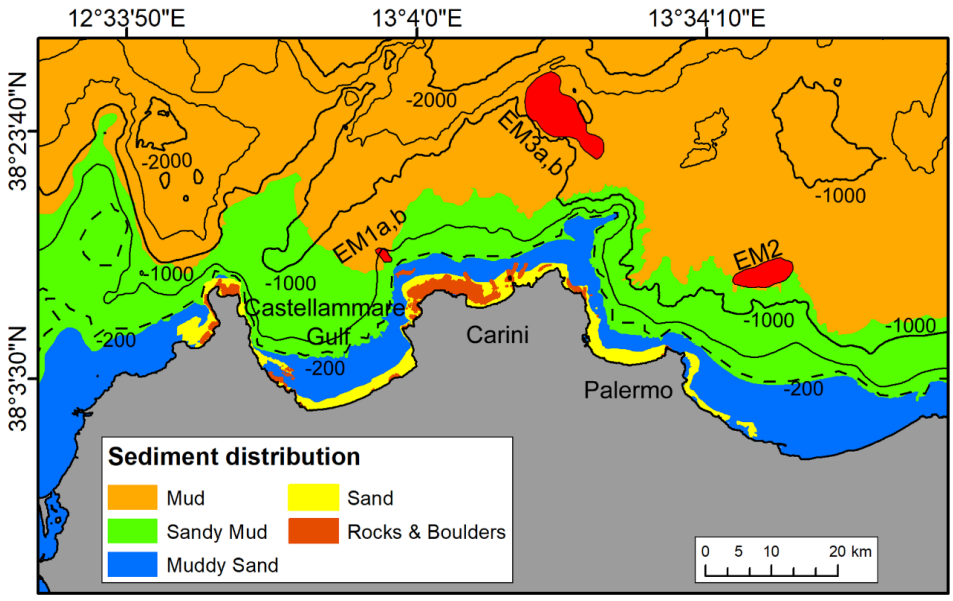


Figure 2. Sediment distribution in the study area (location in Figure 1) (data from Catalano et al. (2013) [48] and EMODnet Geology (https://www.emodnet-geology.eu/, accessed on 15 August 2021). Catalano et al. (2013) [48] collected forty superficial sediment samples in the framework of "CARG Project". The authors carried out a grain size analysis by using sieves, following the ASTM D0422 method and using the laser diffraction particle size technology of "ANALYSETTE 22" by Fritsch [48,49]. The red patches indicate the location of contourite drifts identified in this study. Bathymetry interval: isobaths in black at 500 m intervals from 500 upward, and he dashed line indicates the 200 m isobath (shelf break).

2.2. Oceanographic Setting

The Tyrrhenian Sea is well known for its complex configuration and bathymetry with a strong seasonal variability of the oceanographic processes that are controlled by the water exchange through the Strait of Sicily, the Corsica Channel and the Strait of Sardinia and by local atmospheric fluxes ([50] and references therein). The role of the Straits of Bonifacio, Piombino, and Messina is negligible because the volume of water exchanged is limited.

The study area is dominated by the thermohaline circulation which forms two pathways of east moving water masses: the Modified Atlantic Water (MAW) and the Levantine Intermediate Water (LIW) (Figure 1) [51–55]. The MAW (100–200 m deep layer) originates from inflow in the Mediterranean of the superficial water of the Atlantic Ocean. It undergoes physical and chemical modifications due the water-atmosphere interaction and mixing processes along its path through the Mediterranean Basin [53]. The LIW (200–700 m deep layer) is a water mass that originates in the eastern Mediterranean Sea circulates through both the eastern and western basins and contributes predominantly to the efflux from Gibraltar to the Atlantic [56]. The annual mean speed of the thermohaline-induced currents (LIW and MAW) in the southern Tyrrhenian Sea is ca. 8 m/s [52,57,58].

The water column is also composed in its deeper part by the Tyrrhenian Deep Water (TDW) [54] (Figure 1). The TDW (depth >700 m) is poorly defined as it shows similar characteristics (density >29.08 kg·m^{-3}, temperature over 12.8 °C) to the overlying LIW. Fuda et al. (2002) [59], suggest that the TDW in the north-western Sicilian margin is a mixture of eastern water flowing from the Sicily Channel and western water flowing from the Sardinia Channel.

From a meteo-marine point of view, the study area is affected by sporadic winter storms coming from the NW, NE and E [54] and by seasonal wind-driven currents, defined as the Tyrrhenian Sicilian Current, TSC; [60] with anticyclonic regime, flowing to the west parallel to the coastline with maximum velocities of 0.9 knots [51]. Velocity and direction are highly seasonally variable due to the formation of one or two circulation cells in the Southern Tyrrhenian Sea [51].

3. Data and Methods

The University of Palermo acquired a large set of high resolution bathymetric and seismic data in the study area during three research cruises (2001, 2004, and 2009) on board the research vessels Universitatis (Conisma), Tethis and Minerva 1 (CNR) in the framework of the CARG and MAGIC Projects.

Multibeam bathymetry was derived by merging data acquired using both the Multibeam Reson SeaBat 8111, which generates 105 beams at a frequency of 100 kHz in the depth range of 35–800 m, and the Multibeam Reson SeaBat 8160, which generates 126 beams at a frequency of 50 kHz with depth range of 30–3000 m. In both cases, data positioning was obtained through Differential Global Positioning System; daily record of sound velocity profiles in water column and tidal data were used for data processing. Processing of the multibeam data included elimination of erroneous beams, filtering of noise, processing of navigation data by using the PDS2000 software. Gridding of the filtered soundings was carried out to obtain the final DEM with a 6 m grid size (Figure 3). Multibeam data were integrated with EMODnet bathymetry (http://www.emodnet-bathymetry.eu, accessed on 15 August 2021) (ca. 100 m grid resolution). The processed multibeam data were visualized, analyzed, and interpreted by using Global Mapper and ArcMap 10.2.

About 900 km of high resolution single channel acoustic profiles were acquired using a hull-mounted 16-transducer Teledyne/Benthos CHIRP II profiler (Figure 3). The latter was operated with frequency ranging between 2 and 7 kHz, a ping rate of between 250 and 750 ms, and a pulse length of 10 ms. The sub-bottom data were recorded by using the "Geo-Trace recorder" software by carrying out automatic gain control, time variant gain, swell filtering and muting. The seismic profiles were processed with a conventional single-channel processing sequence that included band pass filtering, gain recovery, seismic signal enhancement, attenuation of noise eddy currents, and seawater column mute [59].

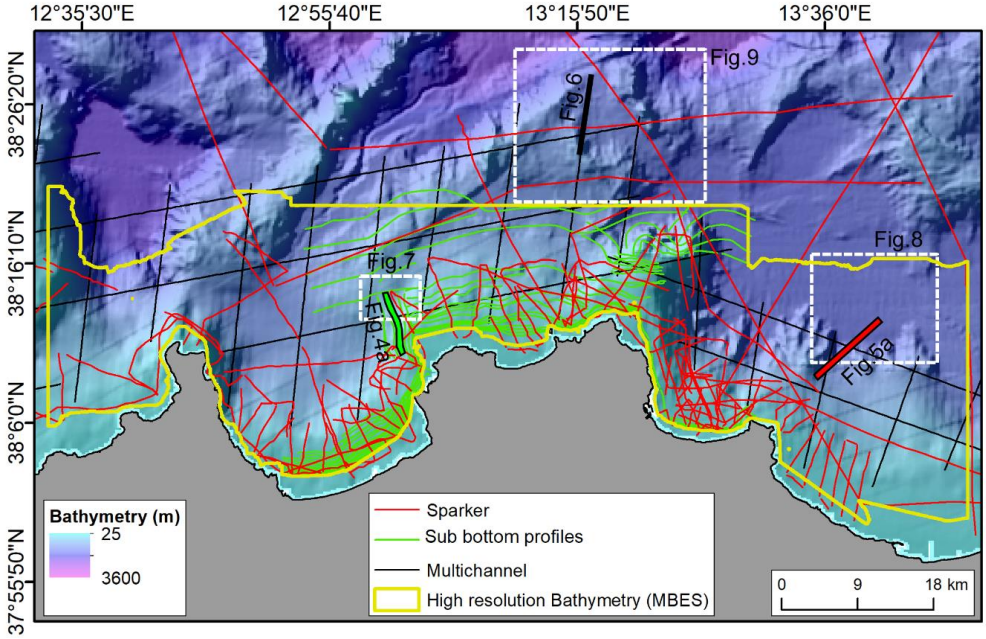


Figure 3. Bathymetric map of the western part of the north-western Sicilian Continental Margin. The map displays the spatial coverage of the marine geology data (multibeam data, sub-bottom profiles CHIRP, Sparker and multichannel seismic reflector profiles). The background bathymetry is from EMODnet bathymetry (http://www.emodnet-bathymetry.eu, accessed on 15 August 2021).

About 750 km of Sparker single-channel seismic profiles were acquired using a 1 kJ and 600–800 Hz Sparker sources. Data processing was performed using the Geo-Suite software, including traces mixing, time variant filters, automatic gain control, time variant gain and spherical divergence correction. Signal penetration was found to exceed 400 ms (TWTT) and the vertical resolution is up to 2.5 m at the seafloor.

In addition, a set of multi-channel seismic reflection profiles characterized by high-penetration (about 6 s, TWTT) and low vertical resolution (10–80 m) were downloaded from the VIDEPI Project database (http://unmig.sviluppoeconomico.gov.it/videpi/, accessed on 15 August 2021) as .pdf files. These seismic lines were georeferenced, and converted to SEG-Y format using a Matlab script (image2segy [61]).

All the profiles were visualized and interpreted using Kingdom suite and GeoSuite Work packages. The reflectors marking the top and bottom of each seismic unit were identified and extracted as horizons in time. Conversion of these horizons to depth was carried out using the following interval velocities: 1500 m/s for the water, 1600 m/s for the Holocene sediments and 1700 m/s for the Plio-Quaternary sedimentary units. Such velocities were derived from lithostratigraphy and sonic log data collected in wells from the western and southern Sicilian offshore [33,62]. The age and seismic character of the Messinian erosional surface and the Messinian sequence were tied to the well-known Messinian seismic markers of the Mediterranean Basin [63,64].

4. Results

The analysis of multibeam and high resolution seismic reflection data (Sub bottom profiler Chirp, Sparker, and airgun-sourced multichannel) from the western part of the north-western Sicilian Continental Margin reveals the presence of five bodies with elongated morphology at the seafloor providing their seismostratigraphic and morphological characters.

4.1. Seismic Stratigraphy and Identification of Elongated Deposits

The sub bottom profile Chirp highlights the occurrence of two elongated mounded deposits (EM1a, b), formed by the shallower seismic unit characterized by mounded

geometry. EM1a, b are located in the upper slope about 10 km off the coastline. EM1a is ca. 1.2 km wide and has a maximum thickness of 45 ms (about 36 m) in its center that thins northwards, ranging in depth from 490 and 550 m. EM1b that is smaller has a maximum thickness of 30 ms (about 24 m) and the same depth range of EM1a. EM1, b is topped by the seafloor and have an asymmetric profile bounded by two small moats (Figure 4a,b). Internally, both the deposits are generally characterized by high amplitude and divergent reflectors, whose frequency strongly increase in the upper part with an internal progradational geometry with downdip terminations (downlap), while the seismic reflectors are truncated by a possible buried moat (Figure 4b).

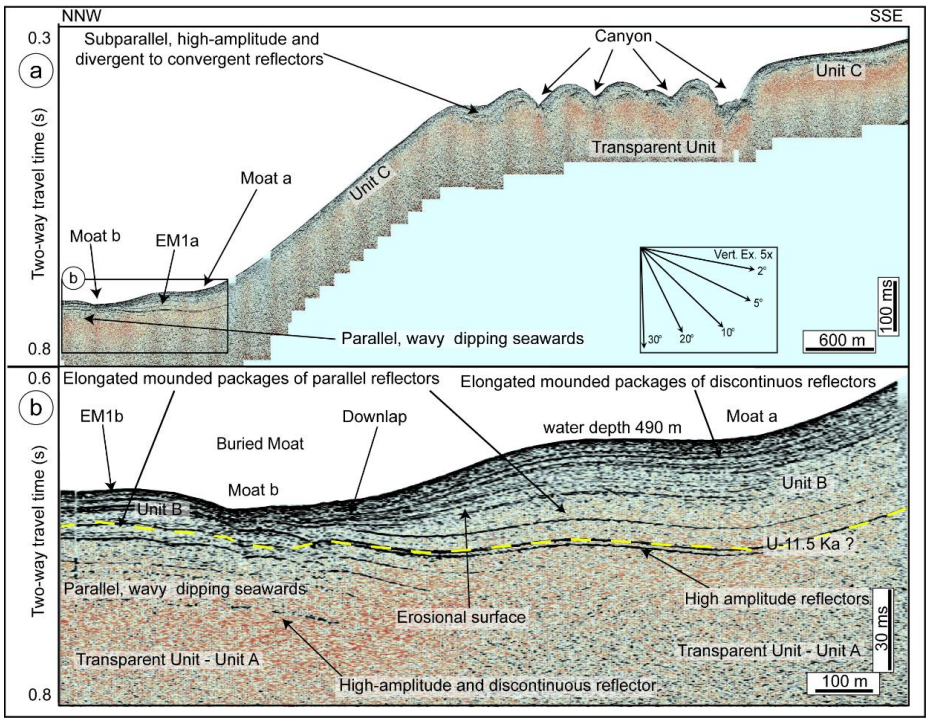


Figure 4. (**a**) Sub bottom profiler Chirp Puma-82 showing the seismic characters of the elongated mounded deposits EM1a, b. (**b**) Zoomed section of Figure 4a. Location of the seismic profiles is shown in Figure 3.

Three main seismic units were distinguished on the basis of seismic facies, internal geometry, and external configuration (Figure 4). The deepest seismic unit (Unit A) is acoustically transparent even if it is difficult to discriminate the lack of reflectors from the loss of penetration of the high-frequency acoustic signal (Figure 4a,b). It mainly occurs in the whole study area and is characterized by seismic facies with high amplitude and high frequency reflectors alternating with transparent intervals. At the top, it is bounded by a wavy couplet of high amplitude and high frequency reflectors (U, dashed yellow line in Figure 4b), which are the base of the uppermost seismic unit with subparallel, high-amplitude and divergent reflectors with good lateral continuity (Unit C in Figure 4a). It is bounded by the seafloor at the top (Figure 4a). It laterally passes to another seismic unit showing elongated mounded packages of sub-parallel, convex upward, continuous reflectors with an aggradation and basinward prograding stratal configuration (Unit B in Figure 4b). Within this unit, an erosional surface is present, bounding a set of high-amplitude, high-continuity reflectors above a set of more transparent (lower amplitude-lower continuity) reflectors below (Figure 4b).

To the east of the Palermo gulf, the single-channel Sparker profile in Figure 5a shows the presence of a third elongated and slightly mounded deposit (EM2) in the upper slope at a depth of ca. 1470 m, about 15 km off the coastline. EM2 is more than 3.7 km wide and has a maximum thickness of 77 ms (about 65 m). EM2 is formed by a seismic unit

C, characterized by an internal aggradational stacking pattern with elongated mounded packages of continuous, moderate to high amplitude reflectors that are locally sub-parallel, undulating or gently folded (Figure 5a,b). It displays relevant vertical and lateral changes in seismic character. The internal seismic character shows continuous high amplitude reflectors dipping landward, alternating with chaotic to transparent seismic facies (Figure 5a,b). The lower boundary of EM2 is a continuous and irregular high amplitude seismic reflector (Figure 5b).

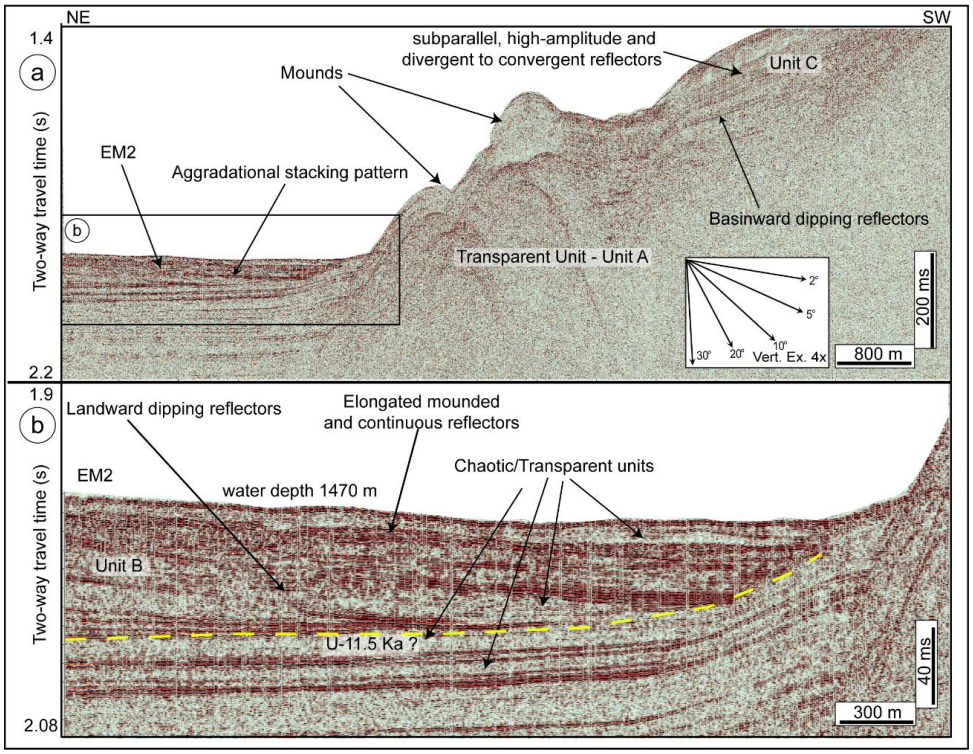


Figure 5. (**a**) Sparker profile P-10 showing the seismic characters of the elongated deposit EM2. (**b**) Zoomed section of Figure 5a. Location of the seismic profiles is shown in Figure 3.

In the central eastern region, others two elongated deposits have been identified by using a multichannel seismic line (EM3a, b in Figure 6). EM3a is more than 6.7 km wide, has a convex shape, and is oriented about NW-SE. It is located at about 25 km off Palermo coastline where the continental shelf is about 5.75 km wide. It has a variable thickness that is up to 410 ms and is equivalent to ca. 350 m, while EM3b that is thinner has a maximum thickness of 280 ms, equivalent to ca. 240 m. EM3a,b internally are made up of wavy intermediate amplitude and/or discontinuous basinward dipping reflectors. The bottom part of the elongated deposits are formed by more irregular and discontinuous reflector with lower amplitude than the upper part (Figure 6) The base of the deposits is marked by a very high amplitude and continuous basinward dipping reflector that for the similar seismic character has been correlated to the Messinian erosional surface described in Lofi et al. (2011) [63] (dashed pink line in Figure 6). Accordingly, EM3a onlaps against deposits that are truncated the Messinian unconformity and are characterized by seismic facies with high amplitude reflectors with poor to good lateral continuity, at times chaotic internal configuration, and evidence of irregular folding probably linked to the post-Messinian tectonics affecting the area (Figure 6).

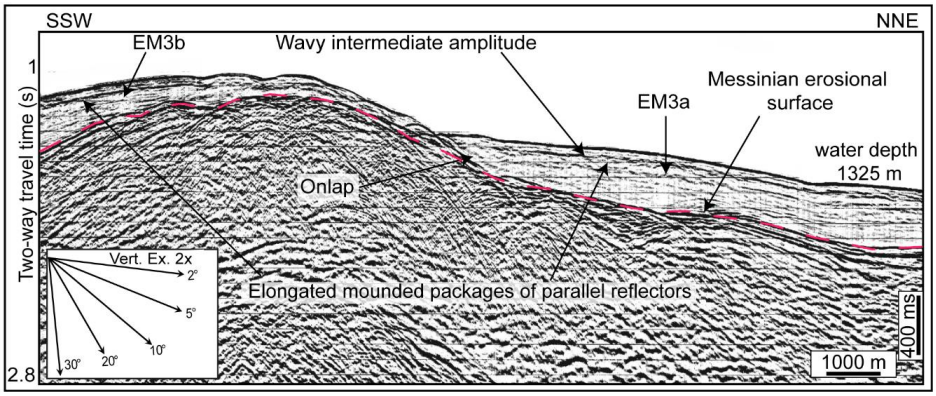


Figure 6. Zoom of multichannel seismic profile crossing the continental slope in the offshore of Palermo, showing EM3 overlapping the Messinian erosional surface marked by a high amplitude reflector [63]. Location of the seismic profile is shown in Figure 3.

4.2. Geomorphological Expression and Characters of Elongated Deposits

EM1a, b are roughly oriented NW-SE, extend for about 3 km sub-parallel to the present north-western Sicilian margin and is rimmed by well-defined moats (Figures 4a,b and 7). EM1a morphologically is up to 30 m high and about 2 km wide and covers an area of 2.5 km^2. EM1b morphologically is up to 25 m high and about 1 km wide (Figure 7a,b). EM1a, b have a moderate gentle (3.8°) slope gradient and are enclosed between the 400 m and 550 m isobaths. Their seaward boundary are defined by a smooth, concave change of slope (Figure 7a,b).

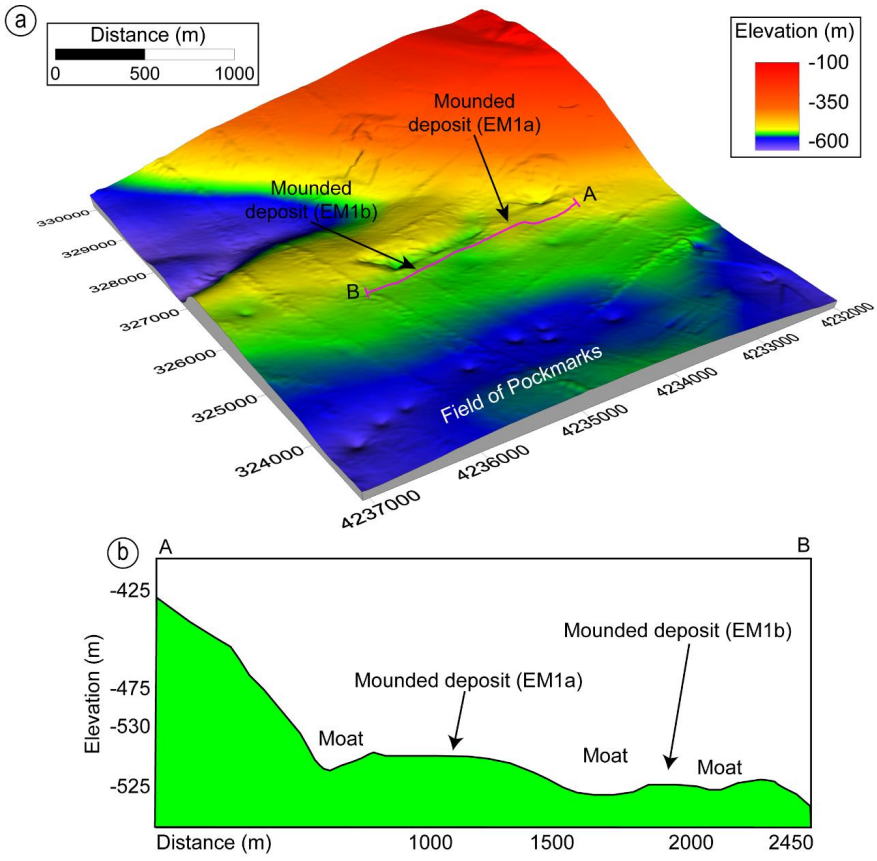


Figure 7. (**a**) Surface 3D multibeam bathymetry of the mounded deposit (EM1a, b). Location of the surface 3D multibeam bathymetry is shown in Figure 3. (**b**) Bathymetric profile across EM1a, b (location in Figure 7a).

EM2 has a very irregular morphology and is more than 9.3 km long. It is oriented about NE-SW and sub-parallel to the present north-western Sicilian margin, located in an intraslope basin at the base of the upper continental slope. EM2 is rimmed by two moats (Figures 5b and 8). EM2 is up to 25 m high and about 3.9 km wide and covers an area of 27 km^2 (Figure 8a,b). EM2 is enclosed between the 1300 m and ca. 1480 m isobaths (Figure 8a,b). The top surface of EM2 shows an uneven morphology that is a prominent characteristic of the seafloor along the Sicilian continental margin.

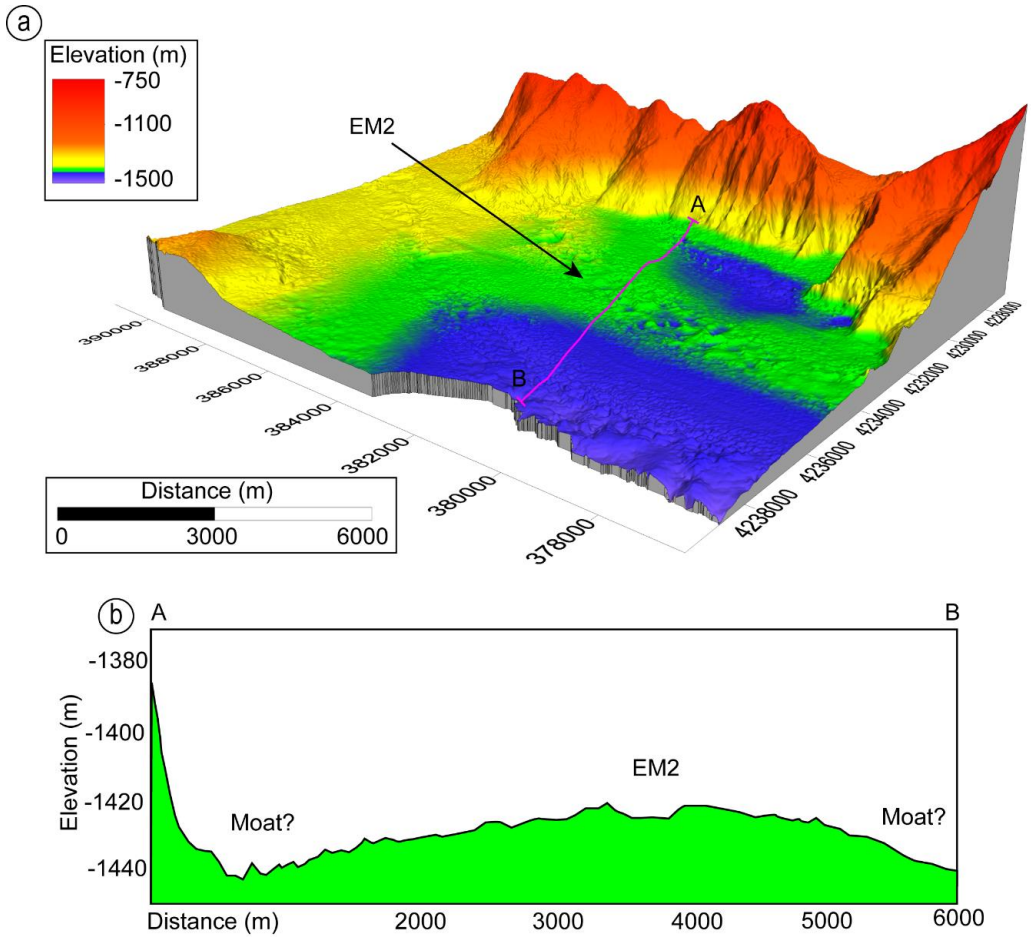


Figure 8. (**a**) Surface 3D multibeam bathymetry of EM2. Location of the surface 3D multibeam bathymetry is shown in Figure 3b. (**b**) Bathymetric profile across EM2 (location in Figure 8a).

EM3a is located outside the area covered by the high resolution multibeam data and for its geomorphological we used the lower resolution bathymetric dataset provided by EMODnet. EM3a is oriented about NW-SE and is more than 16 km long. It is sub-parallel to the current north-western Sicilian margin enclosed between the lower continental slope and a structural high 370 m higher than the surroundings. EM3a is ca. 6 km wide and covers an area of 75 km^2. EM3a has a very gentle slope gradient (up to 3.6°) and is enclosed between the ca. 950 m and 1400 m isobaths (Figure 9).

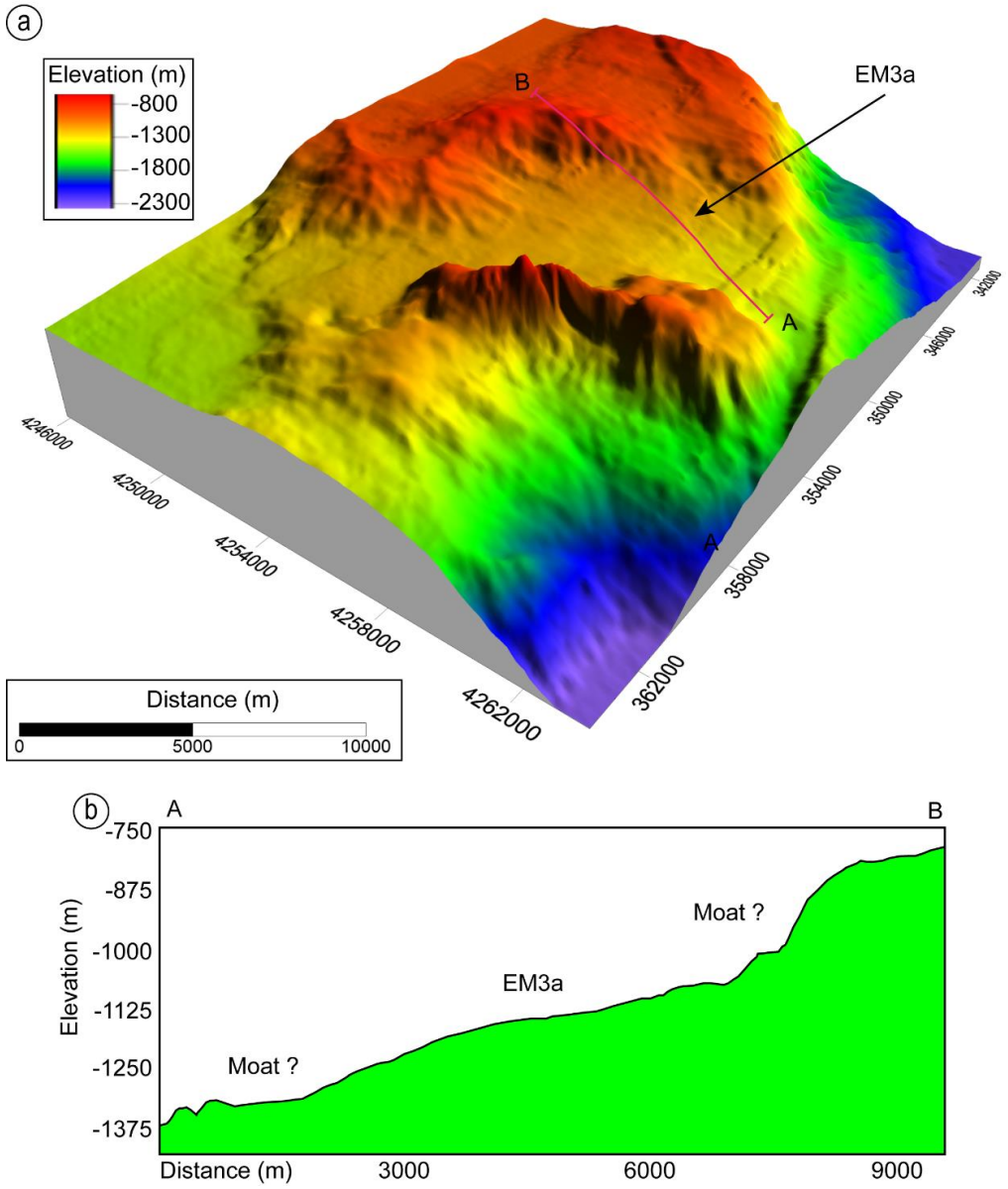


Figure 9. (**a**) Surface 3D multibeam bathymetry of the EM3a. Location of the surface 3D multibeam bathymetry is shown in Figure 3b. (**b**) Bathymetric profile across EM3a (location in Figure 9a).

5. Discussion

5.1. Interpretation of Seismic Facies

The identified seismic facies across the north-western Sicilian Continental Margin have been correlated with published seismic reflection profiles and core data [26,27,33,34,65–67].

The deepest seismic unit showing transparent character mapped by using the sub bottom profile Chirp (Figure 4) and Sparker single-channel seismic profiles (Figure 5) for its high similarity are comparable to the acoustic basement interpreted by Lo Iacono et al. (2011) [34] as composed of Meso-Cenozoic carbonate successions to Tertiary terrigenous sequences corresponding to the rocks outcropping on land.

The seismic unit recognized in the sub bottom profile Chirp (Figure 4) and Sparker single-channel seismic profiles (Figure 5) showing an internal geometry with parallel, wavy or slightly dipping seawards (Figure 4b) has been interpreted as Upper Pleistocene hemipelagic and turbidite deposits according to Sulli et al. (2012) [46].

The well-stratified seismic facies with subparallel, high-amplitude and divergent reflectors (Figures 4a and 5a) has been interpreted as Holocene hemipelagic and turbidite

deposits described along the Sicilian continental margin by Lo Iacono et al. (2014) [31] and Pennino et al. (2014) [63].

The elongated mounded packages of sub-parallel, convex upward reflectors, both continuous and discontinuous (Figures 4a,b, 5a,b and 6), are very similar to those reported along the Tyrrhenian Sea [22,24], Sicily Channel [25–27], and the western Ionian Basin [28,66,68]. Due to this fact and their seismic facies, they have been interpreted as of contouritic origin [1,16,20,69,70].

The basal surfaces of the elongated mounded seismic units mapped by using both sub bottom profile Chirp and Sparker single-channel seismic profiles (U in Figures 4b and 5b) have been interpreted as major erosional truncations, and correlated with the 11.5 ka horizon with origin linked to a minor sea-level fall [65].

EM1-3 considering that are very close to the continental slope could have a genesis linked to the effect of turbidity (and hyperpycnal) flows affecting the local seafloor sedimentation, and they could be interpreted as basin-floor fans and mass-transport deposits. However, EM1-3, considering the high similarity with the contourite drifts documented in the central Mediterranean Region [24,26,27,29], have been interpreted as contourite drift deposits. The scatter plots in Figure 10 shows high similarities in terms of geomorphologic features between EM1-3 and other contourite drifts documented all over the Mediterranean Sea thus strengthening our interpretation (see Table S1 in Supplementary Material; data from http://www.marineregions.org, accessed on 15 August 2021). The scatter plots in Figure 10 display the mapped drifts with respect to the general scaling law of the contourite drifts. The scatter plot a in Figure 10, which relates length and width also highlights the fact that contourite drifts (except EM3a,b) are very small according to their young age and also because they deposited in an active continental margin where the tectonics strongly influence the oceanographic processes of the area.

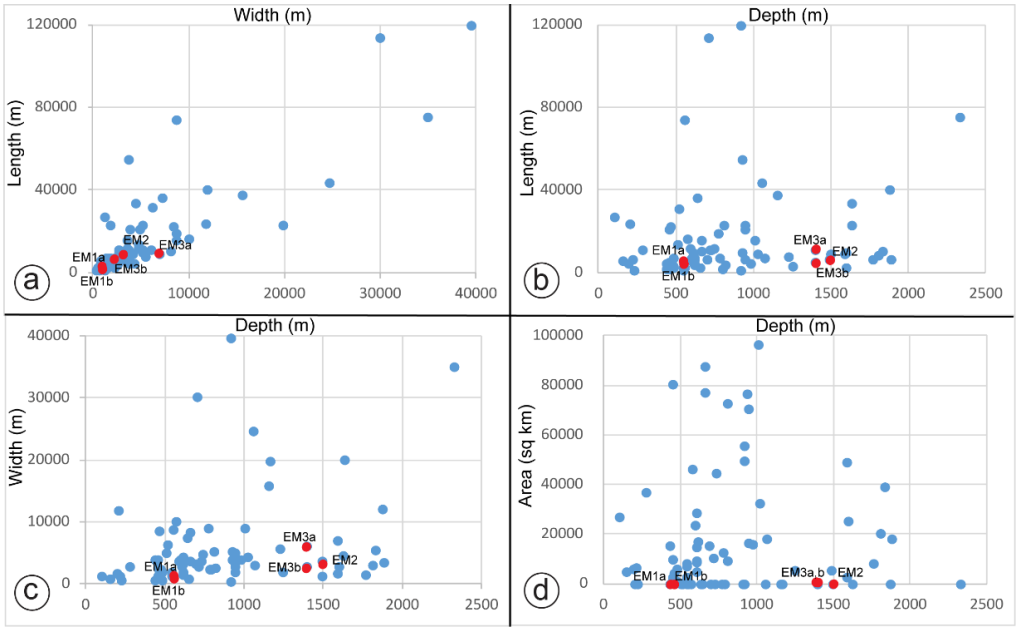


Figure 10. (**a**) the scatter plots of Length and Width; (**b**) the scatter plots of Length and Depth; (**c**) the scatter plots of Width and Depth; (**d**) the scatter plots of Area and Depth. Scatter plots of the physical characters of the NW Sicily contourite drifts compared with other Mediterranean Sea examples. Red dots indicate the contourite drifts described in this manuscript.

5.2. Contourite Drifts in the North-Western Sicilian Margin

EM1a,b have an overall well-defined external geometry of a Moat-Drift-Moat and being similar to that reported to [6,24,71,72] has been interpreted as an Elongated Mounded Drift [1] (Figures 4 and 7). The Chirp profile shows a buried moat (Figure 4b) that is much

more erosive than the present moats at the seafloor. We infer that this feature is due to an earlier period of more vigorous bottom currents and that suggesting also changes in current intensities through time. The bottom circulation was probably more intense in early phases of contourite deposition. This interpretation is also supported by the changing in the vertical seismic characters highlighted by the chirp profile that shows low-continuity reflectors in the shallower part of the drifts.

EM2-3a,b (Figures 5, 6, 8 and 9) due to the absence of a well-defined moat morphology and for their overall geometry and seismic features have been interpreted as sheeted drifts [1]. Recently de Castro et al. (2020) [73] have proposed that contourite drifts are not only made by contourite deposits and hemipelagic settling, and gravity-driven deposits can also contribute in contourite drift aggradation in the Gulf of Cadiz. Alonso et al. (2016) [74] and Miramontes et al. (2016) [32] also proposed similar concepts. In respect of this, we infer that the EM2 on the basis of its seismic character, is composed by a mix of contourite deposits as highlighted by the presence of mounded packages of continuous, moderate to high amplitude reflectors (Figure 5a,b) interbedded with turbiditic and/or mass flow deposits (chaotic/transparent facies in Figure 5b) which are well documented and described by Lo Iacono et al. (2014, 2011) [33,34] and Sulli et al. (2013) [35] along the study area.

The lack of well-defined moats in EM2-3 suggests that in the upper slope the bottom currents were more erosive than in the lower slope, perhaps due to the local complex morphology of the seafloor [33–35].

5.3. Controlling Factors in Contourite Drift Deposition in the North-Western Sicilian Continental Margin

The north-western Sicilian Continental Margin is characterized by six large submarine canyons that are connected to the subaerial fluvial drainage [33,34]. Lo Iacono et al. (2011, 2014) [33,34] have interpreted these canyons as the result of: (i) downslope turbidity currents mainly related to fluvial sedimentary inputs during the last base level fall [28,72,75] and (ii) continuous slope failures as supported by the countless landslide scars. Lo Iacono et al. (2011, 2014) [33,34] proposed a high-energy hydrodynamics scenario affecting the area during the last base level fall when the palaeoshoreline was closer to the shelf edge as also suggested by the general distribution of the outer shelf sandy sediment (Figure 2). Under this scenario, an increase in fluvial sediment supply at the shelf edge/upper slope should be expected and part of the sediment channelized through the canyons and valleys could have formed EM1a, b, EM2.

EM1-3 are located on the slope at different depths between ca. 400 m and ca. 1500 m (Figures 2 and 11). EM1a, b being located at ca. 550 m outcropping on the seafloor have likely been formed by LIW that flows in this area within this depth range (Figure 11). Considering the deeper bathymetry of EM2 and EM3a,b which is between 1000 and 1500 m, we infer that have been formed the by the dense TDW that flows in the area as documented by Fuda et al. (2002) [59] (Figure 11).

The bottom currents that sweep the study area are the LIW and the TDW that play a role in the shaping of the seafloor morphology controlling the deposition of the contourite drifts in the north-western Sicilian Continental Margin (Figure 11).

The dating of contourite drift deposits is difficult as seafloor cores are not available in the drifts. However, a relative chronostratigraphy of the deposits can be inferred based on cores surroundings [65]. EM1 and EM2 develops above the major erosional truncation (U in Figures 4b and 5b) dated as 11.5 ky by Caruso et al. (2011) [65]. Therefore, we propose that the causative bottom currents were active at water depth up to 1600 m since the onset of the Holocene and therefore can be linked to the present-day LIW and TDW. The chronostratigraphic dating of EM3a,b is much more complex especially due to the lower resolution of multichannel seismic line. The only constraint is the bottom of the contourite drift that rest above a high amplitude reflector that has been correlated to the Messinian erosional surface [63,64].

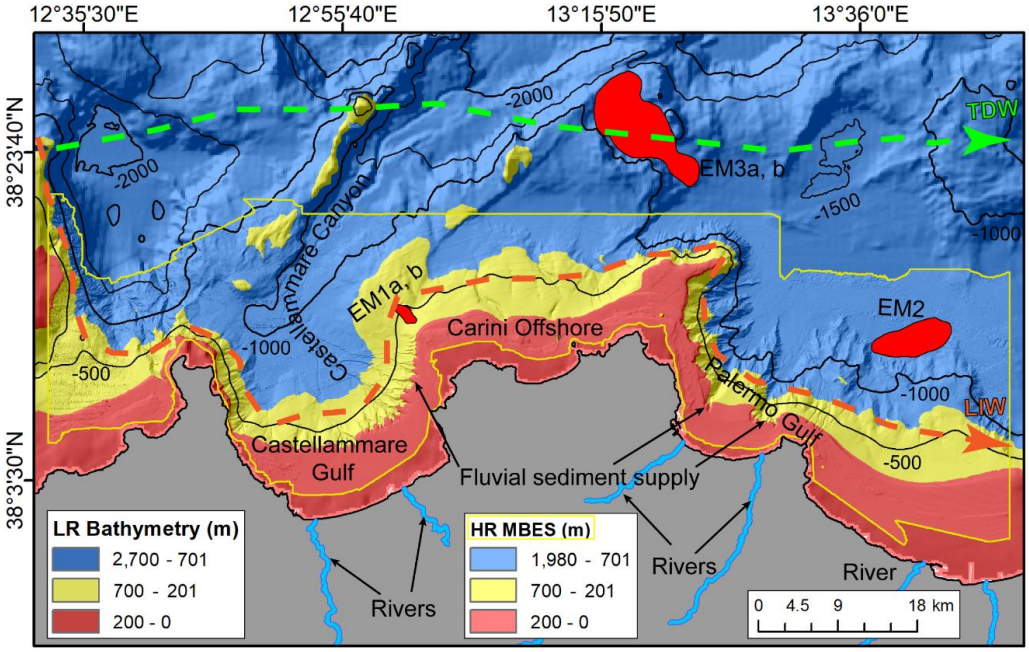


Figure 11. High resolution bathymetric map showing the spatial distribution of the contourite drifts mapped across the study area, and the distribution of main pathways water masses of the north-western Sicilian Continental Margin [51]. The colors used for the bathymetry indicate the domains of the main water masses flowing in the study area. The background bathymetry is from EMODnet bathymetry (http://www.emodnet-bathymetry.eu, accessed on 15 August 2021).

6. Conclusions

Geophysical data from the north-western Sicilian Continental Margin reveals for the first time the occurrence of small contourite drifts and they may contribute to the understanding the important role of the intermediate Mediterranean waters in the sedimentary evolution and palaeoceanographic changes in the north-western Sicilian Continental Margin. Our main conclusions are the following:

Two different kinds of contourite drifts, at different range of bathymetry, have been documented along the upper and lower continental slope of the north-western Sicilian Continental Margin.

The mapped contourite drift (except EM3) are patchy with small width and thickness because of their young age and because they occur in an active continental margin where the tectonics plays a relevant role in the shaping an uneven seafloor morphology which is dominated by several canyons.

Two elongated mounded drifts (EM1a,b) formed by a mix of Holocene hemipelagic sediments deposited at the top of an erosional truncation aged at 11.5 ka [65] are located at a water depth of ca. 570m. It is possible that energy of the fluxes decreased through the time.

Three sheeted drifts (EM2, EM3a,b) deposited at the toe of the upper continental slope. EM2 is internally composed by a mix of contourite deposits interbedded with turbiditic and mass flow deposits possibly fed through the canyons.

Supplementary Materials: The following are available online at https://www.mdpi.com/article/10.3390/jmse9101043/s1. Table S1. Geomorphologic features all over the Mediterranean Sea.

Author Contributions: Conceptualization, D.S. and A.S.; methodology, D.S. and A.S.; validation, D.S.; formal analysis, D.S. and A.S.; investigation, D.S. and A.S.; data curation, A.S.; writing original draft preparation, D.S.; writing review and editing, A.S., D.C. and F.L.C.; visualization, D.S.; supervision, A.S.; project administration, A.S.; funding acquisition, A.S. All authors have read and agreed to the published version of the manuscript.

Funding: This research received no external funding.

Institutional Review Board Statement: Not applicable.

Informed Consent Statement: Not applicable.

Data Availability Statement: The data used to support the findings of this study are available from A.S. attilio.sulli@unipa.it and from the corresponding author upon request.

Acknowledgments: We wish to acknowledge colleagues from the Department of Earth and Marine Sciences of the University of Palermo for their contribution to the research work. Geophysical data were acquired as part of the CARG project, funded by the Italian National Geological Survey (ISPRA), and MaGIC project (Marine Geological Hazard along the Italian Coast), funded by the Italian Civil Protection Department. We are grateful to the captains of the R/Vs and all relative crews for their help during data acquisition and onboard operations. All participants and technical staff from the oceanographic cruises are gratefully acknowledged for their contribution to the research work.

Conflicts of Interest: The authors declare no conflict of interest.

References

1. Rebesco, M.; Hernández-Molina, F.J.; Van Rooij, D.; Wåhlin, A. Contourites and associated sediments controlled by deep-water circulation processes: State-of-the-art and future considerations. *Mar. Geol.* **2014**, *352*, 111–154. [CrossRef]
2. Hernández-Molina, F.J.; Wåhlin, A.; Bruno, M.; Ercilla, G.; Llave, E.; Serra, N.; Rosón, G.; Puig, P.; Rebesco, M.; Van Rooij, D. Oceanographic processes and morphosedimentary products along the Iberian margins: A new multidisciplinary approach. *Mar. Geol.* **2016**, *378*, 127–156. [CrossRef]
3. Rebesco, M.; Camerlenghi, A. *Contourites*; Elsevier: Amsterdam, The Netherlands, 2008; ISBN 9780444529985.
4. Rebesco, M.; Özmaral, A.; Urgeles, R.; Accettella, D.; Lucchi, R.G.; Rüther, D.; Winsborrow, M.; Llopart, J.; Caburlotto, A.; Lantzsch, H. Evolution of a high-latitude sediment drift inside a glacially-carved trough based on high-resolution seismic stratigraphy (Kveithola, NW Barents Sea). *Quat. Sci. Rev.* **2016**, *147*, 178–193. [CrossRef]
5. Hanebuth, T.J.J.; Zhang, W.; Hofmann, A.L.; Löwemark, L.A.; Schwenk, T. Oceanic density fronts steering bottom-current induced sedimentation deduced from a 50 ka contourite-drift record and numerical modeling (off NW Spain). *Quat. Sci. Rev.* **2015**, *112*, 207–225. [CrossRef]
6. Miramontes, E.; Garreau, P.; Caillaud, M.; Jouet, G.; Pellen, R.; Hernández-Molina, F.J.; Clare, M.A.; Cattaneo, A. Contourite distribution and bottom currents in the NW Mediterranean Sea: Coupling seafloor geomorphology and hydrodynamic modelling. *Geomorphology* **2019**, *333*, 43–60. [CrossRef]
7. Ercilla, G.; Juan, C.; Hernandez-Molina, F.J.; Bruno, M.; Estrada, F.; Alonso, B.; Casas, D.; lí Farran, M.; Llave, E.; Garcia, M. Significance of bottom currents in deep-sea morphodynamics: An example from the Alboran Sea. *Mar. Geol.* **2016**, *378*, 157–170. [CrossRef]
8. Faugères, J.C.; Stow, D.A.V.; Imbert, P.; Viana, A. Seismic features diagnostic of contourite drifts. *Mar. Geol.* **1999**, *162*, 1–38. [CrossRef]
9. Rebesco, M.; Wåhlin, A.; Laberg, J.S.; Schauer, U.; Beszczynska-Möller, A.; Lucchi, R.G.; Noormets, R.; Accettella, D.; Zarayskaya, Y.; Diviacco, P. Quaternary contourite drifts of the Western Spitsbergen margin. *Deep Res. Part I Oceanogr. Res. Pap.* **2013**, *79*, 156–168. [CrossRef]
10. Esentia, I.; Stow, D.; Smillie, Z. Contourite drifts and associated bedforms. In *Submarine Geomorphology*; Springer: Cham, Switzerland, 2018; pp. 301–331.
11. Heezen, B.C.; Hollister, C.D.; Ruddiman, W.F. Shaping of the continental rise by deep geostrophic contour currents. *Science* **1966**, *152*, 502–508. [CrossRef]
12. Nutz, A.; Lajeunesse, P.; Ghienne, J.-F.; Schuster, M.; Brouard, E.; Dietrich, P.; Bouchette, F.; Roquin, C.; Cousineau, P.A. Deglacial to paraglacial history of the Lake Saint-Jean Lowlands: A geomorphological perspective. In *Landscapes and Landforms of Eastern Canada. World Geomorphological Landscapes*; Slaymaker, S.O., Catto, N., Eds.; Springer: Cham, Switzerland, 2020; ISBN 978-3-030-35137-3.
13. Juan, C.; Ercilla, G.; Estrada, F.; Alonso, B.; Casas, D.; Vázquez, J.T.; d'Acremont, E.; Medialdea, T.; Hernández-Molina, F.J.; Gorini, C. Multiple factors controlling the deep marine sedimentation of the Alboran Sea (SW Mediterranean) after the Zanclean Atlantic Mega-flood. *Mar. Geol.* **2020**, *423*, 106138. [CrossRef]
14. Viana, A.R. Economic relevance of contourites. *Dev. Sedimentol.* **2008**, *60*, 491–510.
15. Yu, X.; Stow, D.; Smillie, Z.; Esentia, I.; Brackenridge, R.; Xie, X.; Bankole, S.; Ducassou, E.; Llave, E. Contourite porosity, grain size and reservoir characteristics. *Mar. Pet. Geol.* **2020**, *117*, 104392. [CrossRef]
16. Laberg, J.S.; Camerlenghi, A.; Rebesco, M. *Chapter 25 The Significance of Contourites for Submarine Slope Stability*; Rebesco, M., Camerlenghi, A., Eds.; Elsevier: Amsterdam, The Netherlands, 2008; ISBN 9780444529985.
17. Cattaneo, A.; Miramontes, E.; Samalens, K.; Garreau, P.; Caillaud, M.; Marsset, B.; Corradi, N.; Migeon, S. Contourite identification along Italian margins: The case of the Portofino drift (Ligurian Sea). *Mar. Pet. Geol.* **2017**, *87*, 137–147. [CrossRef]

18. Solheim, A.; Berg, K.; Forsberg, C.F.; Bryn, P. The Storegga Slide complex: Repetitive large scale sliding with similar cause and development. *Mar. Pet. Geol.* **2005**, *22*, 97–107. [CrossRef]
19. Kane, I.A.; Clare, M.A.; Miramontes, E.; Wogelius, R.; Rothwell, J.J.; Garreau, P.; Pohl, F. Seafloor microplastic hotspots controlled by deep-sea circulation. *Science* **2020**, *368*, 1140–1145. [CrossRef] [PubMed]
20. Stow, D.A.V.; Faugères, J.C.; Howe, J.A.; Pudsey, C.J.; Viana, A.R. Bottom currents, contourites and deep-sea sediment drifts: Current state-of-the-art. *Geol. Soc. Mem.* **2002**, *22*, 7–20. [CrossRef]
21. Juan, C.; Ercilla, G.; Hernández-Molina, F.J.; Estrada, F.; Alonso, B.; Casas, D.; García, M.; Llave, E.; Palomino, D.; Vázquez, J.-T. Seismic evidence of current-controlled sedimentation in the Alboran Sea during the Pliocene and Quaternary: Palaeoceanographic implications. *Mar. Geol.* **2016**, *378*, 292–311. [CrossRef]
22. Martorelli, E.; Petroni, G.; Chiocci, F.L.; Bosman, A.; Calarco, M.; Conte, A.M.; Macelloni, L.; Salusti, E.; Sposato, A. Contourites offshore Pantelleria Island (Sicily Channel, Mediterranean Sea): Depositional, erosional and biogenic elements. *Geo-Mar. Lett.* **2011**, *31*, 481–493. [CrossRef]
23. Verdicchio, G.; Trincardi, F. Mediterranean shelf-edge muddy contourites: Examples from the Gela and South Adriatic basins. *Geo-Mar. Lett.* **2008**, *28*, 137–151. [CrossRef]
24. Martorelli, E.; Falcini, F.; Salusti, E.; Chiocci, F.L. Analysis and modeling of contourite drifts and contour currents off promontories in the Italian Seas (Mediterranean Sea). *Mar. Geol.* **2010**, *278*, 19–30. [CrossRef]
25. Ferraro, S.; Sulli, A.; Di Stefano, E.; Giaramita, L.; Incarbona, A.; Graham Mortyn, P.; Sprovieri, M.; Sprovieri, R.; Tonielli, R.; Vallefuoco, M.; et al. Late Quaternary palaeoenvironmental reconstruction of sediment drift accumulation in the Malta Graben (central Mediterranean Sea). *Geo-Mar. Lett.* **2018**, *38*, 241–258. [CrossRef]
26. Spatola, D.; Micallef, A.; Sulli, A.; Basilone, L.; Ferreri, R.; Basilone, G.; Bonanno, A.; Pulizzi, M.; Mangano, S. The Graham Bank (Sicily Channel, central Mediterranean Sea): Seafloor signatures of volcanic and tectonic controls. *Geomorphology* **2018**, *318*, 375–389. [CrossRef]
27. Micallef, A.; Foglini, F.; Le Bas, T.; Angeletti, L.; Maselli, V.; Pasuto, A.; Taviani, M. The submerged paleolandscape of the maltese Islands: Morphology, evolution and relation to quaternary environmental change. *Mar. Geol.* **2013**, *335*, 129–147. [CrossRef]
28. Micallef, A.; Camerlenghi, A.; Georgiopoulou, A.; Garcia-Castellanos, D.; Gutscher, M.-A.; Lo Iacono, C.; Huvenne, V.A.I.; Mountjoy, J.J.; Paull, C.K.; Le Bas, T.; et al. Geomorphic evolution of the Malta Escarpment and implications for the Messinian evaporative drawdown in the eastern Mediterranean Sea. *Geomorphology* **2019**, *327*, 264–283. [CrossRef]
29. Amelio, M.; Martorelli, E. Seismo-stratigraphic characters of paleocontourites along the Calabro-Tyrrhenian margin (Southern Tyrrhenian Sea). *Mar. Geol.* **2008**, *252*, 141–149. [CrossRef]
30. Marani, M.; Argnani, A.; Roveri, M.; Trincardi, F. Sediment drifts and erosional surfaces in the central Mediterranean: Seismic evidence of bottom-current activity. *Sediment. Geol.* **1993**, *82*, 207–220. [CrossRef]
31. Martorelli, E.; Italiano, F.; Ingrassia, M.; Macelloni, L.; Bosman, A.; Conte, A.M.; Beaubien, S.E.; Graziani, S.; Sposato, A.; Chiocci, F.L. Evidence of a shallow water submarine hydrothermal field off Zannone Island from morphological and geochemical characterization: Implications for Tyrrhenian Sea Quaternary volcanism. *J. Geophys. Res. Solid Earth* **2016**, *121*, 8396–8414. [CrossRef]
32. Miramontes, E.; Cattaneo, A.; Jouet, G.; Thereau, E.; Thomas, Y.; Rovere, M.; Cauquil, E.; Trincardi, F. The Pianosa contourite depositional system (northern Tyrrhenian Sea): Drift morphology and Plio-Quaternary stratigraphic evolution. *Mar. Geol.* **2016**, *378*, 20–42. [CrossRef]
33. Lo Iacono, C.; Sulli, A.; Agate, M. Submarine canyons of North-western Sicily (Southern Tyrrhenian Sea): Variability in morphology, sedimentary processes and evolution on a tectonically active margin. *Deep Res. Part II Top. Stud. Oceanogr.* **2014**, *104*, 93–105. [CrossRef]
34. Iacono, C.L.; Sulli, A.; Agate, M.; Lo Presti, V.; Pepe, F.; Catalano, R. Submarine canyon morphologies in the Gulf of Palermo (Southern Tyrrhenian Sea) and possible implications for geo-hazard. *Mar. Geophys. Res.* **2011**, *32*, 127–138. [CrossRef]
35. Sulli, A.; Agate, M.; Iacono, C.L.; Presti, V.L.; Pennino, V.; Polizzi, S. Submarine slope failures along the northern sicilian continental margin (Southern Tyrrhenian Sea) and possible implications for geo-hazard. In *Proceedings of the Landslide Science and Practice*; Spinger: Berlin/Heidelberg, Germany, 2013; pp. 41–48.
36. Spatola, D.; Micallef, A.; Sulli, A.; Basilone, L.; Basilone, G. Evidence of active fluid seepage (AFS) in the southern region of the central Mediterranean Sea. *Measurement* **2018**, *128*, 247–253. [CrossRef]
37. Pepe, F.; Sulli, A.; Bertotti, G.; Catalano, R. Structural highs formation and their relationship to sedimentary basins in the north Sicily continental margin (southern Tyrrhenian Sea): Implication for the Drepano Thrust Front. *Tectonophysics* **2005**, *409*, 1–18. [CrossRef]
38. Sulli, A.; Zizzo, E.; Albano, L. Comparing methods for computation of run-up heights of landslide-generated tsunami in the Northern Sicily continental margin. *Geo-Mar. Lett.* **2018**, *38*, 439–455. [CrossRef]
39. Kastens, K.; Mascle, J.; Auroux, C.; Bonatti, E.; Broglia, C.; Channell, J.; Curzi, P.; Emeis, K.C.; Glačon, G.; Hasegawa, S.; et al. ODP Leg 107 in the Tyrrhenian Sea: Insights into passive margin and back-arc basin evolution. *Bull. Geol. Soc. Am.* **1988**, *100*, 1140–1156. [CrossRef]
40. Bonardi, G.; De Capoa, P.; Staso, A.D.; Estévez, A.; Martín-Martín, M.; Martín-Rojas, I.; Perrone, V.; Tent-Manclús, J.E. Oligocene-to-early miocene depositional and structural evolution of the Calabria-Peloritani Arc southern terrane (Italy) and geodynamic correlations with the Spain betics and Morocco rif. *Geodin. Acta* **2003**, *16*, 149–169. [CrossRef]

41. Catalano, R.; Valenti, V.; Albanese, C.; Accaino, F.; Sulli, A.; Tinivella, U.; Morticelli, M.G.; Zanolla, C.; Giustiniani, M. Sicily's fold–thrust belt and slab roll-back: The SI. RI. PRO. seismic crustal transect. *J. Geol. Soc.* **2013**, *170*, 451–464. [CrossRef]
42. Chiarabba, C.; De Gori, P.; Speranza, F. The southern Tyrrhenian subduction zone: Deep geometry, magmatism and Plio-Pleistocene evolution. *Earth Planet. Sci. Lett.* **2008**, *268*, 408–423. [CrossRef]
43. Doglioni, C.; Harabaglia, P.; Merlini, S.; Mongelli, F.; Peccerillo, A.; Piromallo, C. Orogens and slabs vs. their direction of subduction. *Earth Sci. Rev.* **1999**, *45*, 167–208. [CrossRef]
44. Faccenna, C.; Piromallo, C.; Crespo-Blanc, A.; Jolivet, L.; Rossetti, F. Lateral slab deformation and the origin of the western Mediterranean arcs. *Tectonics* **2004**, *23*. [CrossRef]
45. Catalano, R.; D'argenio, B.; Montanari, L.; Morlotti, E.; Torelli, L. Marine geology of the NW Sicily offshore (Sardinia Channel) and its relationships with mainland structures. *Boll. Soc. Geol. Ital.* **1985**, *104*, 207–215.
46. Sulli, A.; Agate, M.; Mancuso, M.; Pepe, F.; Pennino, V.; Polizzi, S.; Presti, V.L.; Gargano, F.; Interbartolo, F. Variability of depositional setting along the North-western Sicily continental shelf (Italy) during Late Quaternary: Effects of sea level changes and tectonic evolution. *Alp. Mediterr. Quat* **2012**, *25*, 141–155.
47. Agate, M.; Catalano, R.; Infuso, S.; Lucido, M.; Mirabile, L.; Sulli, A. Structural evolution of the northern Sicily continental margin during the Plio-Pleistocene. *Geol. Dev. Sicil. Platf.* **1993**, *58*, 25–30.
48. Catalano, R.; Basilone, L.; Di Maggio, C.; Gasparo Morticelli, M.; Agate, M.; Avellone, G. *Note Illustrative della Carta Geologica del Foglio n. 594–585 "Partinico-Mondello" (Scala 1:50.000) della Carta Geologica D'Italia e Carta Geologica Allegata*; ISPRA Istituto Superiore per la Protezione e la Ricerca Ambientale: Rome, Italy, 2013.
49. Catalano, R.; Avellone, G.; Basilone, L.; Contino, A.; Agate, M.; Di Maggio, C.; Lo Iacono, C.; Sulli, A.; Gugliotta, C.; Gasparo Morticelli, M. *Carta Geologica D'Italia Alla Scala 1:50.000 E Note Illustrative del Foglio 595_Palermo*; ISPRA, Servizio Geologico D'Italia: Rome, Italy, 2013.
50. de la Vara, A.; Parras-Berrocal, I.; Izquierdo, A.; Sein, D.; Cabos, W. Climate change signal in the ocean circulation of the Tyrrhenian Sea. *Earth Syst. Dyn. Discuss.* **2021**, 1–27.
51. Istituto Idrografico della Marina. *Atlante della Correnti Superficiali dei Mari Italiani*; Istituto Idrografico della Marina: Genoa, Italy, 1982.
52. Millot, C. Circulation in the western Mediterranean Sea. *J. Mar. Syst.* **1999**, *20*, 423–442. [CrossRef]
53. Pinardi, N.; Masetti, E. Variability of the large scale general circulation of the Mediterranean Sea from observations and modelling: A review. *Palaeogeogr. Palaeoclimatol. Palaeoecol.* **2000**, *158*, 153–173. [CrossRef]
54. Astraldi, M.; Gasparini, G.P.; Vetrano, A.; Vignudelli, S. Hydrographic characteristics and interannual variability of water masses in the central Mediterranean: A sensitivity test for long-term changes in the Mediterranean Sea. *Deep Sea Res. Part I Oceanogr. Res. Pap.* **2002**, *49*, 661–680. [CrossRef]
55. Volkov, D.L.; Baringer, M.; Smeed, D.; Johns, W.; Landerer, F.W. Teleconnection between the Atlantic meridional overturning circulation and sea level in the Mediterranean Sea. *J. Clim.* **2019**, *32*, 935–955. [CrossRef]
56. Robinson, A.R.; Leslie, W.G.; Theocharis, A.; Lascaratos, A. Mediterranean Sea circulation. *Encycl. Ocean Sci.* **2001**, *1*, 19. [CrossRef]
57. Millot, C. The circulation of the Levantine Intermediate Water in the Algerian basin. *J. Geophys. Res. Ocean.* **1987**, *92*, 8265–8276. [CrossRef]
58. Astraldi, M.; Gasparini, G.P.; Gervasio, L.; Salusti, E. Dense water dynamics along the Strait of Sicily (Mediterranean Sea). *J. Phys. Oceanogr.* **2001**, *31*, 3457–3475. [CrossRef]
59. Fuda, J.; Etiope, G.; Millot, C.; Favali, P.; Calcara, M.; Smriglio, G.; Boschi, E. Warming, salting and origin of the Tyrrhenian Deep Water. *Geophys. Res. Lett.* **2002**, *29*, 1–4. [CrossRef]
60. Menna, M.; Poulain, P.-M.; Ciani, D.; Doglioli, A.; Notarstefano, G.; Gerin, R.; Rio, M.-H.; Santoleri, R.; Gauci, A.; Drago, A. New insights of the Sicily Channel and southern Tyrrhenian Sea variability. *Water* **2019**, *11*, 1355. [CrossRef]
61. Farran, M. IMAGE2SEGY: Una aplicación informática para la conversión de imágenes de perfiles sísmicos a ficheros en formato SEG Y. *Geo-Temas* **2008**, *10*, 1215–1218.
62. Catalano, R.; Franchino, A.; Merlini, S.; Sulli, A. Central western Sicily structural setting interpreted from seismic reflection profiles. *Mem. Soc. Geol. Ital.* **2000**, *55*, 5–16.
63. Lofi, J.; Déverchère, J.; Gaullier, V.; Gillet, H.; Gorini, C.; Guennoc, P.; Loncke, L.; Maillard, A.; Sage, F.; Thinon, I.; et al. *Seismic Atlas of the Messinian Salinity Crisis markers in the Mediterranean and Black Seas*; Mémoires de la Société Géologique de France: Paris, France, 2011.
64. Lofi, J. *Seismic Atlas of the Messinian Salinity Crisis markers in the Mediterranean Sea—Volume 2*; Société Géologique de France: Paris, France, 2018; Volume 181.
65. Caruso, A.; Cosentino, C.; Pierre, C.; Sulli, A. Sea-level changes during the last 41,000 years in the outer shelf of the southern Tyrrhenian Sea: Evidence from benthic foraminifera and seismostratigraphic analysis. *Quat. Int.* **2011**, *232*, 122–131. [CrossRef]
66. Spatola, D.; del Moral-Erencia, J.D.; Micallef, A.; Camerlenghi, A.; Garcia-Castellanos, D.; Gupta, S.; Bohorquez, P.; Gutscher, M.A.; Bertoni, C. A single-stage megaflood at the termination of the Messinian salinity crisis: Geophysical and modelling evidence from the eastern Mediterranean Basin. *Mar. Geol.* **2020**, *430*, 106337. [CrossRef]
67. Pennino, V.; Sulli, A.; Caracausi, A.; Grassa, F.; Interbartolo, F. Fluid escape structures in the north Sicily continental margin. *Mar. Pet. Geol.* **2014**, *55*, 202–213. [CrossRef]

68. Rebesco, M.; Camerlenghi, A.; Munari, V.; Mosetti, R.; Ford, J.; Micallef, A.; Facchin, L. Bottom current-controlled quaternary sedimentation at the foot of the Malta Escarpment (Ionian Basin, Mediterranean). *Mar. Geol.* **2021**, *441*, 106596. [CrossRef]
69. Ercilla, G.; Casas, D.; Iglesias, J.; Vázquez, J.T.; Somoza, L.; León, R.; Medialdea, T.; Juan, C.; García, M. *Contourites in the Galicia Bank Region (NW Iberian Atlantic)*; Sociedad Geológica de España: Salamanca, Spain, 2010.
70. Rebesco, M.; Stow, D. Seismic expression of contourites and related deposits: A preface. *Mar. Geophys. Res.* **2001**, *22*, 303–308. [CrossRef]
71. Hernández-Molina, F.J.; Paterlini, M.; Somoza, L.; Violante, R.; Arecco, M.A.; De Isasi, M.; Rebesco, M.; Uenzelmann-Neben, G.; Neben, S.; Marshall, P. Giant mounded drifts in the Argentine Continental Margin: Origins, and global implications for the history of thermohaline circulation. *Mar. Pet. Geol.* **2010**, *27*, 1508–1530. [CrossRef]
72. Micallef, A.; Mountjoy, J.J.; Barnes, P.M.; Canals, M.; Lastras, G. Geomorphic response of submarine canyons to tectonic activity: Insights from the Cook Strait canyon system, New Zealand. *Geosphere* **2014**, *10*, 905–929. [CrossRef]
73. de Castro, S.; Hernandez-Molina, F.J.; Rodríguez-Tovar, F.J.; Llave, E.; Ng, Z.L.; Nishida, N.; Mena, A. Contourites and bottom current reworked sands: Bed facies model and implications. *Mar. Geol.* **2020**, *428*, 106267. [CrossRef]
74. Alonso, B.; Ercilla, G.; Casas, D.; Stow, D.A.V.; Rodríguez-Tovar, F.J.; Dorador, J.; Hernández-Molina, F.-J. Contourite vs. gravity-flow deposits of the Pleistocene Faro Drift (Gulf of Cadiz): Sedimentological and mineralogical approaches. *Mar. Geol.* **2016**, *377*, 77–94. [CrossRef]
75. Gerber, T.P.; Amblas, D.; Wolinsky, M.A.; Pratson, L.F.; Canals, M. A model for the long-profile shape of submarine canyons. *J. Geophys. Res. Earth Surf.* **2009**, *114*, 1–24. [CrossRef]